



Contents lists available at ScienceDirect

Clinical and Translational Radiation Oncology

journal homepage: www.elsevier.com/locate/ctro

Review Article

Technical design and concept of a 0.35 T MR-Linac

Sebastian Klüter

Department of Radiation Oncology, University Hospital Heidelberg, Heidelberg Institute for Radiation Oncology (HIRO), National Center for Radiation Research in Oncology (NCRO), Heidelberg, Germany



ARTICLE INFO

Article history:

Received 30 March 2019

Revised 5 April 2019

Accepted 6 April 2019

Available online 8 April 2019

ABSTRACT

The integration of magnetic resonance (MR) imaging and linear accelerators into hybrid treatment systems has made MR-guided radiation therapy a clinical reality. This work summarizes the technical design of a 0.35 T MR-Linac and corresponding clinical concepts. The system facilitates 3D-conformal as well as IMRT treatments with 6MV photons. Daily MR imaging provides superior soft-tissue contrast for patient setup and also enables on-table adaption of treatment plans, which is fully integrated into the treatment workflow of the system. Automated beam gating during delivery is facilitated by cine MR imaging and structure tracking. Combining different novel features compared to conventional image-guided radiotherapy, this technology offers the potential for margin reduction as well as dose escalation.

© 2019 The Author. Published by Elsevier B.V. on behalf of European Society for Radiotherapy and Oncology. This is an open access article under the CC BY-NC-ND license (<http://creativecommons.org/licenses/by-nc-nd/4.0/>).

1. Introduction

Hybrid devices combining magnetic resonance (MR) imaging with radiation therapy (RT) delivery have recently been introduced. Four different systems for photon MR-guided radiotherapy (MRgRT) are being developed, using different magnetic field strengths and orientations of the static magnetic field to the treatment beam [1–4]. The ViewRay MRIdian Linac (ViewRay Inc., Oakwood, USA) integrates a 0.35 T split superconducting magnet (double-donut) with a 6 MV flattening-filter-free (FFF) linear accelerator. A previous version of the ViewRay MRIdian system used three Co-60 heads instead of a linac [4] and has been in clinical use since 2014 [5,6], while the first patients have been treated with the linac version of the system in 2017 [7]. The MR unit of the system enables pre- and post-treatment MR imaging (MRI) of a patient and thus offers the potential of improved target localization due to a superior soft-tissue contrast compared to standard image-guided radiotherapy techniques [8]. Furthermore, on-table plan adaptation based on actual locations of target and organs at risk as visualized by the MRI can be performed. During the treatment, cine MRI in one or three sagittal planes can be used for automated beam control (gating) [9]. Here, the design characteristics and specifications of the ViewRay MRIdian Linac system are described and the corresponding concepts for clinical use are being outlined (Fig. 1).

2. System design

The MRIdian Linac system houses a 0.35 T split superconducting magnet with a 28 cm gap between the two magnet halves. For stability reasons, both halves are mechanically and thermally connected [10]. The circular gantry assembly holding all linac components is placed at the gap between both magnet halves, such that the treatment beam is emitted perpendicular to the static magnetic field [7]. Because the gradient coil is also split and narrows to a 5 mm thick connecting fiberglass part at the magnet gap, the treatment beam is exposed to little attenuating material. Starting at 33°, the radiation gantry can be set to any beam angle as far as 30°; due to technical limitations, angles between 30° and 33° are not available. The gradient system shows a gradient strength of 18 mT m⁻¹ and a slew rate of 200 T/m/s [11]. The overall MR imaging unit of the MRIdian Linac remained largely unchanged compared to the previous cobalt-version of the system [4].

Since the linear accelerator could not function properly in the presence of a static magnetic field, six shielding compartments (so-called buckets) are mounted upon the gantry, which contain the linac as well as linac components, for example the magnetron (see Fig. 2) [10]. Each compartment consists of a number of concentric ferromagnetic cylinders, effectively shielding their inside from the magnetic field. Furthermore, the shielding compartments also provide radiofrequency (RF) shielding, so that the MR imaging is not disturbed by the RF noise generated due to linac operation. The RF shielding is implemented via layers of RF absorbing carbon fiber and RF reflecting copper.

E-mail address: sebastian.klueter@med.uni-heidelberg.de

<https://doi.org/10.1016/j.ctro.2019.04.007>

2405-6308/© 2019 The Author. Published by Elsevier B.V. on behalf of European Society for Radiotherapy and Oncology. This is an open access article under the CC BY-NC-ND license (<http://creativecommons.org/licenses/by-nc-nd/4.0/>).



Fig. 1. Photograph of the MRIdian Linac system that has been installed at Heidelberg University Hospital in 2017.

Both MRI and linac share the same isocenter. Room lasers are installed with the system, projecting to a virtual isocenter outside the bore which is usually located at 155 cm distance to the treatment isocenter. The overall targeting accuracy of the MRIdian Linac has been evaluated by Wen et al. [10] by means of a phantom with MR/CT properties and containing a Winston-Lutz cube. They found the end-to-end localization accuracy of the system to be 1.0 ± 0.1 mm.

The bore of the system is 70 cm wide. Within the bore restrictions, the patient couch can be moved in all three dimensions, enabling the correction of setup errors by couch shifts [12]. Possible couch heights range from 20 cm below the isocenter up to isocenter, while possible lateral movements depend on the actual couch height. The maximum lateral movement at sufficient couch height amounts to ± 7 cm and decreases with lower couch heights. During treatment planning, the achievable couch positions can be displayed and taken into account for isocenter placement.

2.1. Linac and MLC

The linac operates in the S-band and generates a 6 MV FFF photon beam with a dose rate of 600 cGy/min at a source-to-axis distance (SAD) of 90 cm. The treatment beam is shaped by a double-stack, double-focus multi-leaf collimator (MLC) without additional

jaws, and the virtual focusing point of the MLC lies 15 mm above the focal spot of the linac. In total, the MLC consists of 138 tungsten alloy leaves distributed among the two stacks. Each stack has a physical leaf height of 5.5 cm, so that the total MLC leaf height amounts to 11 cm. The leaf sides are flat without any tongue or groove. In order to minimize leakage radiation at the focusing leaf sides, the two MLC stacks are shifted against each other by half a leaf width. Since the width of a single leaf is 8.3 mm at the isocentric plane, the resulting effective leaf width amounts to 4.15 mm. All leaves allow full interdigitation and overtravel and move in the IEC-X direction. The minimum programmable field size is 0.2×0.415 cm², and the maximum field size is 27.4×24.1 cm². While no detailed dosimetric characterization has yet been published, Bohoudi et al. [13] have presented an analysis of the achievable treatment plan quality using this MLC.

2.2. MR imaging

The MR imaging unit of the system provides a 50 cm diameter spherical field of view (DSV). It uses a whole-body RF transmit coil [4] and surface receive coils anterior and posterior of the patient [14]. The receive coils consist of radiolucent phased arrays with 2×5 channels (anterior and posterior) for head and neck and 2×6 channels for the torso, are embedded in low-density foam and show uniform attenuating characteristics [4].

The pulse sequence used for volumetric imaging as well as cine MRI in the clinical mode of the system is a True Fast Imaging with Steady State Precession (TRUFI) sequence, which is a type of balanced steady-state free precession (bSSFP) sequence, yielding a T_2/T_1 -weighted contrast [9,15]. For volumetric imaging, the user can choose between predefined field of views (FOVs) with an in-plane resolution of 1.5 mm \times 1.5 mm and slice thicknesses of 1.5 mm and 3 mm. Two-dimensional cine MR images can be acquired continuously in one sagittal plane at four frames/s or in three sagittal planes at two frames/s, also during treatment. For cine MR, also predefined FOVs can be chosen, and the in-plane resolution is 3.5 mm \times 3.5 mm with slice thicknesses of 5 mm, 7 mm or 10 mm. Additional pulse sequences can be used in research mode and for Quality Assurance (QA) [16,17], and have also been used in studies by different research groups using MRIdian cobalt-systems [18–20].

Because the MRI is used for target localization and beam control, geometric distortions in the MR images need to be characterized, and high spatial integrity is important for precise targeting [17]. The vendor-defined specifications for geometric accuracy are 1 mm within a 20 cm DSV and 2 mm within a 35 cm DSV. Using a vendor-supplied cuboid 2D spatial integrity phantom of 30×30

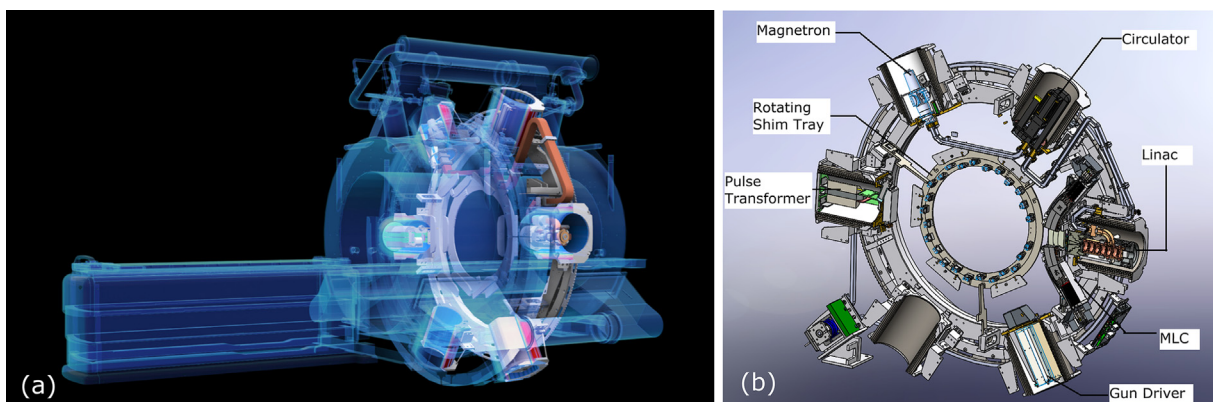


Fig. 2. (a) Schematic drawing of the system depicting the main hardware components: superconducting double-donut magnet, circular radiation gantry and patient couch; (b) schematic drawing of the radiation gantry with linac components and MLC. Images courtesy of ViewRay Inc.

cm² size, Nejad-Davarani et al. [17] have assessed distortions at a MRIdian Linac and reported mean total distortions of <0.8 mm with maximum distortions of 1.41/0.99/1.56 mm in axial/coronal/sagittal planes, respectively. They also found that while distortions were negligible within a 20 cm DSV, larger distortions of several millimeters occurred outside the 35 cm DSV, especially towards the border of the maximum FOV of the system [17].

3. Treatment planning and delivery

The treatment planning system (TPS) is fully integrated into the treatment delivery software and shares the same patient database. Treatment plans can be created for 3D conformal RT as well as step-and-shoot intensity-modulated RT (IMRT). Inverse treatment plan optimization is implemented by means of fluence map optimization with subsequent leaf sequencing. The optimization algorithm itself employs convex penalty functions for all voxels, which can be weighted against each other according to their associated structures. Dose calculation is always performed by a fast Monte Carlo dose calculation algorithm with the option to take the static magnetic field into account. MR simulation scans as well as computed tomography (CT) scans can be used as primary images for treatment planning [6]. Both can be rigidly or deformably registered in order to support multi-modality contouring and as well for electron density propagation, if MR scans are chosen as primary images. Furthermore, bulk density assignments can be performed using custom densities as well as 6 pre-defined densities for different types of tissue. Within the system software, bulk density assignments are the only current option in the case of MR-only treatment planning.

3.1. On-table treatment plan adaption

The system allows on-table adaption of treatment plans based on daily MR treatment setup scans. Conceptually, the workflow for online adaptive RT (ART) in the treatment delivery software remains unchanged compared to the cobalt-version of the system. Each daily scan is registered to the primary planning image, and initial planning contours as well as electron density information can be rigidly copied or deformed to it. The deformed contours can be fine-tuned or recontoured if necessary, and the original treatment plan can then be recalculated on the daily anatomy and corresponding contours [6,21–23]. Based on comparison of the predicted daily dose distribution to the originally planned dose distribution, the user can choose to either treat with the original plan or to adapt the treatment plan. Plan adaption can be performed as segment-weight optimization, fluence reoptimization using original planning objectives or full reoptimization with modified objectives [6,12,21–23]. While it is possible to check and recontour all structures [23], Bohoudi et al. [22] have described an approach of limiting checks and corrections of daily contours to an area within 3 cm of the surface of the target volume, which should usually be the region of highest dose gradients. Using the cobalt-version of the system, they have reported an average time of 12 ± 4.5 min per patient for the overall adaptive process including contour review and adjustment and plan reoptimization [22]. Lamb et al. [23] have reported a median time of 24 min per patient for re-contouring, plan adaptation and online QA, also using the cobalt system.

Since no verification measurement for QA of an on-table adapted treatment plan can be performed, the system provides a secondary Monte Carlo dose calculation, that can as well account for the magnetic field. The software automatically generates a report comparing both original and secondary dose calculation in terms of dose-volume-histogram (DVH) parameters as well as

gamma analysis. Additionally, the vendor-supplied QA tool also compares the original treatment plan to the reoptimized daily plan regarding number of segments, segment shapes and weights, and Monitor Units [6,22–24]. After delivery, the system generates a report containing a delivery record as well as an evaluation of recorded Monitor Units and MLC leaf positions compared to the planned values. Furthermore, delivered dose can be recalculated using the information recorded in the machine delivery log files, and the log files can be also exported [25].

The vendor-supplied online QA approach is limited by the fact that the secondary Monte Carlo tool uses a beam model equivalent to the TPS [23]. Moreover, a secondary dose calculation is not able to identify all potential errors during on-table plan adaption. Cai et al. [26] have conducted a comprehensive risk analysis for online ART and implemented a QA program accordingly, which includes additional manual evaluations as well as automated checks, for example an in-house developed plan quality and -integrity checking software tool. Lamb et al. [23] have also reported on automated plan consistency checks for online ART.

3.2. Cine MR-enabled anatomy tracking and beam gating

During RT delivery, the system can gate the beam automatically by use of cine MRI and online structure tracking in the live images. The gating concept has been described in detail by Green et al. [9]. Briefly, a gating target structure is defined by the user in a sagittal slice of the volumetric MRI, as well as the desired gating margin and percentage of the target allowed outside the margin before beam shut-off. Right before start of treatment, a preview cine MRI scan is acquired. This is used by the system for automated selection of a tracking key frame based on deformable image registration of a certain number of preview frames to the corresponding slice of the volumetric scan. During treatment, the live cine MRI frames are in turn deformably registered to the key frame, and based on that deformation the gating target is deformed. If in any frame the target is outside the specified margin and allowed “target out” percentage, the beam will be shut off. This concept allows for free-breathing gating [9] as well as gating using repeated breath-holds [27,28].

In order to visually guide patients especially for repeated breath-holds, some authors have reported on in-room screens or projectors [28,29]. During RT delivery, the patients can thereby see their live cine MR images including projections of target and margin, and thus actively control their breathing.

For accurate delivery of gated treatments, the overall gating latency of the system is important. For the cobalt-version of the system, average gating latencies ranging from about 300 ms to about 436 ms have been reported [6,9,27]. The vendor-defined specification for gating latency of the MRIdian Linac system is <500 ms. While it has been hypothesized that the linac system could enable faster beam hold than the cobalt-version of the system, where a shutter has to mechanically close [30], no published data are yet available for the linac system.

4. Conclusion

The MRIdian Linac is a hybrid system for low-field MRgRT. Compared to conventional RT, three prominent features can be identified: (i) superior soft-tissue imaging contrast due to the integration of MRI, (ii) the possibility of on-table adaption of treatment plans, and (iii) the option to use cine MRI for intrafraction target tracking and automated beam gating. While on-table adaption has already been broadly discussed in a non-MR-guided context, it was often limited by image quality or FOV of on-table imaging modalities. Using MRI, it seems possible to overcome those limita-

tions. Thus, together with the fully integrated adaptive workflow, the system enables a comprehensive online adaptive strategy [8]. Combined with the use of MR-enabled gating during treatment delivery, which does not need any external surrogates or implanted fiducial markers, the technology offers the potential for margin reduction as well as dose escalation [8,22,31,32].

Conflict of interest

The author has received travel reimbursement and honoraria from ViewRay Inc. No financial support was received for the submitted work.

Acknowledgment

This work was kindly supported by the German Research Foundation (DFG).

References

- [1] Legendijk JJ, Raaymakers BW, van Vulpen M. The magnetic resonance imaging-linac system. *Semin Radiat Oncol* 2014;24:207–9.
- [2] Fallone BG. The rotating biplanar linac-magnetic resonance imaging system. *Semin Radiat Oncol* 2014;24:200–2.
- [3] Keall PJ, Barton M, Crozier S. The Australian magnetic resonance imaging-linac program. *Semin Radiat Oncol* 2014;24:203–6.
- [4] Mutic S, Dempsey JF. The ViewRay system: magnetic resonance-guided and controlled radiotherapy. *Semin Radiat Oncol* 2014;24:196–9.
- [5] Olsen J, Green O, Kashani R. World's first application of MR-guidance for radiotherapy. *Mo Med* 2015;112:358–60.
- [6] Acharya S, Fischer-Valuck BW, Kashani R, et al. Online magnetic resonance image guided adaptive radiation therapy: first clinical applications. *Int J Radiat Oncol Biol Phys* 2016;94:394–403.
- [7] Liney GP, Whelan B, Oborn B, et al. MRI-linear accelerator radiotherapy systems. *Clin Oncol (Royal College of Radiologists (Great Britain))* 2018;30:686–91.
- [8] Kashani R, Olsen JR. Magnetic resonance imaging for target delineation and daily treatment modification. *Semin Radiat Oncol* 2018;28:178–84.
- [9] Green OL, Rankine LJ, Cai B, et al. First clinical implementation of real-time, real anatomy tracking and radiation beam control. *Med Phys* 2018.
- [10] Wen N, Kim J, Doemer A, et al. Evaluation of a magnetic resonance guided linear accelerator for stereotactic radiosurgery treatment. *Radiother Oncol* 2018;127:460–6.
- [11] Paganelli C, Whelan B, Peroni M, et al. MRI-guidance for motion management in external beam radiotherapy: current status and future challenges. *Phys Med Biol* 2018;63:22tr03.
- [12] Pathmanathan AU, van As NJ, Kerkmeijer LGW, et al. Magnetic resonance imaging-guided adaptive radiation therapy: a “game changer” for prostate treatment? *Int J Radiat Oncol Biol Phys* 2018;100:361–73.
- [13] Bohoudi O, Palacios MA, Slotman BJ, et al. OC-0519: radiotherapy plan quality using a double focused, double stacked multi-leaf collimator. *Radiother Oncol* 2018;127:S273.
- [14] Acharya S, Fischer-Valuck BW, Mazur TR, et al. Magnetic resonance image guided radiation therapy for external beam accelerated partial-breast irradiation: evaluation of delivered dose and intrafractional cavity motion. *Int J Radiat Oncol Biol Phys* 2016;96:785–92.
- [15] Bieri O, Scheffler K. Fundamentals of balanced steady state free precession MRI. *J Magn Reson Imaging* 2013;38:2–11.
- [16] Hu Y, Rankine L, Green OL, et al. Characterization of the onboard imaging unit for the first clinical magnetic resonance image guided radiation therapy system. *Med Phys* 2015;42:5828–37.
- [17] Nejad-Davarani SP, Kim JP, Du D, Glide-Hurst C. Large field of view distortion assessment in a low-field MR-linac. *Med Phys* 2019.
- [18] Yang Y, Cao M, Sheng K, et al. Longitudinal diffusion MRI for treatment response assessment: preliminary experience using an MRI-guided tri-cobalt 60 radiotherapy system. *Med Phys* 2016;43:1369–73.
- [19] Shaverdian N, Yang Y, Hu P, et al. Feasibility evaluation of diffusion-weighted imaging using an integrated MRI-radiotherapy system for response assessment to neoadjuvant therapy in rectal cancer. *Br J Radiol* 2017;90:20160739.
- [20] Gao Y, Han F, Zhou Z, et al. Distortion-free diffusion MRI using an MRI-guided Tri-Cobalt 60 radiotherapy system: sequence verification and preliminary clinical experience. *Med Phys* 2017;44:5357–66.
- [21] Henke L, Kashani R, Robinson C, et al. Phase I trial of stereotactic MR-guided online adaptive radiation therapy (SMART) for the treatment of oligometastatic or unresectable primary malignancies of the abdomen. *Radiother Oncol* 2018;126:519–26.
- [22] Bohoudi O, Bruynzeel AME, Senan S, et al. Fast and robust online adaptive planning in stereotactic MR-guided adaptive radiation therapy (SMART) for pancreatic cancer. *Radiother Oncol* 2017;125:439–44.
- [23] Lamb J, Cao M, Kishan A, et al. Online adaptive radiation therapy: implementation of a new process of care. *Cureus* 2017;9.
- [24] Yang D, Wooten HO, Green O, et al. A software tool to automatically assure and report daily treatment deliveries by a cobalt-60 radiation therapy device. *J Appl Clin Med Phys* 2016;17:492–501.
- [25] Li HH, Rodriguez VL, Green OL, et al. Patient-specific quality assurance for the delivery of (60)Co intensity modulated radiation therapy subject to a 0.35-T lateral magnetic field. *Int J Radiat Oncol Biol Phys* 2015;91:65–72.
- [26] Cai B, Green OL, Kashani R, et al. A practical implementation of physics quality assurance for photon adaptive radiotherapy. *Z Med Phys* 2018;28:211–23.
- [27] Lamb JM, Ginn JS, O'Connell DP, et al. Dosimetric validation of a magnetic resonance image gated radiotherapy system using a motion phantom and radiochromic film. *J Appl Clin Med Phys* 2017;18:163–9.
- [28] van Sorsen de Koste JR, Palacios MA, Bruynzeel AME, et al. MR-guided gated stereotactic radiation therapy delivery for lung, adrenal, and pancreatic tumors: a geometric analysis. *Int J Radiat Oncol Biol Phys* 2018;102:858–66.
- [29] Kim JJ, Lee H, Wu HG, et al. Development of patient-controlled respiratory gating system based on visual guidance for magnetic-resonance image-guided radiation therapy. *Med Phys* 2017;44:4838–46.
- [30] Mittauer K, Paliwal B, Hill P, et al. A new era of image guidance with magnetic resonance-guided radiation therapy for abdominal and thoracic malignancies. *Cureus* 2018;10.
- [31] Henke LE, Olsen JR, Contreras JA, et al. Stereotactic MR-guided online adaptive radiation therapy (SMART) for ultracentral thorax malignancies: results of a phase 1 trial. *Adv Radiat Oncol* 2019;4:201–9.
- [32] Luterstein E, Cao M, Lamb J, et al. Stereotactic MRI-guided adaptive radiation therapy (SMART) for locally advanced pancreatic cancer: a promising approach. *Cureus* 2018;10.